Carcinogenesis vol.29 no.8 pp.1639–1647, 2008
doi:10.1093/carcin/bgn155
Advance Access publication June 25, 2008

Aberrant iNOS signaling is under genetic control in rodent liver cancer and potentially prognostic for the human disease

Diego F.Calvisi, Federico Pinna, Sara Ladu, Rossella Pellegrino, Maria R.Muroni, Maria M.Simile, Maddalena Frau, Maria L.Tomasi, Maria R.De Miglio, Maria A.Seddaiu, Lucia Daino, Valeria Sanna, Francesco Feo* and Rosa M.Pascale

Department of Biomedical Sciences, Division of Experimental Pathology and Oncology, University of Sassari, 07100 Sassari, Italy

*To whom correspondence should be addressed. Tel: +39 070228307; Fax: +39 070228485;
Email: feo@uniss.it

Mounting evidence underlines the role of inducible nitric oxide synthase (iNOS) in hepatocellular carcinoma (HCC) development, but its functional interactions with pathways involved in HCC progression remain uninvestigated. Here, we analyzed in preneoplastic and neoplastic livers from Fisher 344 and Brown Norway rats, possessing different genetic predisposition to HCC, in transforming growth factor-α (TGF-α) and c-Myc–TGF-α transgenic mice, characterized by different susceptibility to HCC, and in human HCC: (i) iNOS function and interactions with nuclear factor-kB (NF-kB) and Ha-RAS/extracellular signal-regulated kinase (ERK) during hepatocarcinogenesis; (ii) influence of genetic predisposition to liver cancer on these pathways and role of these cascades in determining a susceptible or resistant phenotype and (iii) iNOS prognostic value in human HCC. We found progressive i*Nos* induction in rat and mouse liver lesions, always at higher levels in the most aggressive models represented by HCC of rats genetically susceptible to hepatocarcinogenesis and c-Myc–TGF-α transgenic mice. iNOS, inhibitor of kB kinase/NF-kB and RAS/ERK upregulation was significantly higher in HCC with poorer prognosis (as defined by patients' survival length) and positively correlated with tumor proliferation, genomic instability and microvascularization and negatively with apoptosis. Suppression of iNOS signaling by aminoguanidine led to decreased HCC growth and NF-kB and RAS/ERK expression and increased apoptosis both *in vivo* and *in vitro*. Conversely, block of NF-kB signaling by sulfasalazine or short interfering RNA (siRNA) or ERK signaling by UO126 caused iNOS downregulation in HCC cell lines. These findings indicate that iNOS cross talk with NF-kB and Ha-RAS/ERK cascades influences HCC growth and prognosis, suggesting that key component of iNOS signaling could represent important therapeutic targets for human HCC.

Introduction

Hepatocellular carcinoma (HCC) is one of the most frequent and deadliest human cancers worldwide. Current therapies do not improve significantly the prognosis of patients with unresectable HCC (1,2). This emphasizes the need to investigate the molecular mechanisms responsible for HCC development to identify new targets for early diagnosis, chemoprevention and treatment.

Abbreviations: AG, aminoguanidine; BN, Brown Norway; ERK, extracellular signal-regulated kinase; F344, Fisher 344; GS2, Glyco-SNAP-2; GTP, guanosine triphosphate; HCC, hepatocellular carcinoma; HCCB, hepatocellular carcinoma with better prognosis; HCCP, hepatocellular carcinoma with poorer prognosis; IFN-γ, interferon-γ; IKB, inhibitor of kB; IKK, inhibitor of kB kinase; IL, interleukin; iNOS, inducible nitric oxide synthase; mRNA, messenger RNA; MVD, microvessel density; NF-kB, nuclear factor-kB; NO•, nitric oxide; pRb, retinoblastoma protein; siRNA, short interfering RNA; SL, surrounding liver; Sulfa, sulfasalazine; TGF-α, transforming growth factor-α; TNF-α, tumor necrosis factor-α.

Numerous genes regulating susceptibility to HCC and controlling growth, progression and redifferentiation of preneoplastic and neoplastic lesions have been mapped in rodents (3). Decrease in growth ability and/or marked redifferentiation of preneoplastic lesion characterizes rodent strains resistant to hepatocarcinogenesis (3,4). Consequently, studies on the mechanisms underlying the acquisition of a phenotype susceptible/resistant to hepatocarcinogenesis in rodent strains, carrying preneoplastic lesions differently prone to progress to HCC, may lead to the discovery of prognostic markers and therapeutic targets for the human disease. Dysplastic nodules and HCC induced in susceptible Fisher 344 (F344) rats show upregulation of *c-Myc*, *Cyclin D1*, *E* and *A* and *E2f1* genes, increased cyclin D1–Cdk4, cyclin E–Cdk2 and E2f1–Dp1 complexes and retinoblastoma protein (pRb) hyperphosphorylation (4–6). These changes are absent or less pronounced in liver lesions from resistant Brown Norway (BN) rats, where a block of G_1–S transition occurs. Interestingly, alterations similar to those of F344 rats also occur in aggressive HCCs from c-Myc–transforming growth factor-α (TGF-α) double-transgenic mice (7) and human hepatocellular carcinoma with poorer prognosis (HCCP) (8), whereas the expression patterns in HCCs from BN rats roughly resemble those of human hepatocellular carcinoma with better prognosis (HCCB). This suggests that the basic mechanisms of hepatocarcinogenesis are similar in rodents and humans (4,7).

Inducible nitric oxide synthase (iNOS) produces sustained nitric oxide (NO•) concentrations in response to proinflammatory agents. NO• is a major mediator of chronic inflammation and may modulate tumorigenesis by regulating cell proliferation, survival, migration, angiogenesis, drug resistance and DNA repair (9–11). In particular, iNOS might promote unrestrained cell growth via its ability to inactivate the retinoblastoma (pRb) pathway (9). NO• effects depend on its concentration and its interaction with other free radicals, metal ions, proteins and cell type that it targets (11). Thus, NO• can both activate the p53-suppressive pathway and induce oncogenic mutations in the p53 gene (11,12). Some observations envisage a cross talk between iNos and inhibitor of kB kinase (IKK)/nuclear factor-kB (NF-kB) and RAS/extracellular signal-regulated kinase (ERK) pathways. The IKK complex and NF-kB activities are strongly reduced in *iNos* knockout mice (12). NO• activates Ha-RAS/ERK pathway in T lymphocytes (13). Phosphorylated ERK activates *iNOS* in melanoma (14) and *NF-kB* in HeLa cells (15). Although the role of NO• has been defined in inflammatory cells, chronic inflammation, oxidative damage, usually associated with viral hepatitis and HCC, and elevated NO• plasma levels are present in patients with cirrhosis and HCC (16); the regulation of NO• production and interactions of iNOS with signaling pathways in hepatocarcinogenesis remain poorly investigated. iNOS, NF-kB, RAS and ERK are upregulated in preneoplastic rat liver lesions (17), dysplastic and neoplastic liver from c-Myc–TGF-α transgenic mice (18) and human HCCs (19,20), but the functional interactions between iNOS, NF-kB and Ha-RAS/ERK signaling and their role in HCC predisposition, development and progression have never been proved. Furthermore, their prognostic role has not been evaluated.

To address this issue, we analyzed in preneoplastic and neoplastic liver lesions differently prone to progression, induced in rats and mice with different predisposition to HCC, and in human HCC subtypes with different prognosis: (i) the role of the interactions of iNOS with IKK/NF-kB and Ha-RAS/ERK signaling during different stages of hepatocarcinogenesis; (ii) the influence of genetic or molecular predisposition to HCC on these pathways and their role in determining a phenotype susceptible or resistant to HCC and (iii) the potential prognostic significance of changes in iNOS/IKK/NF-kB and iNOS/Ha-RAS/ERK signaling in human HCC.

Materials and methods

Tissue specimens, cell lines and treatments

F344 and BN rats were fed, housed and treated according to the 'resistant hepatocyte' protocol (21) including a 150 mg/kg intraperitoneal dose of diethylnitrosamine followed by 15 days feeding of a 0.02% 2-acetylaminofluorene containing hyperprotein diet, with a partial hepatectomy at the midpoint of this feeding. Rats were killed by bleeding through thoracic aorta, under ether anesthesia, and preneoplastic liver (4–12 weeks after initiation), nodules (32 weeks) and HCCs (57–60 weeks) were collected and used for experiments. Generation of MT/TGF-α single-transgenic (TGF-α) and Alb/c-Myc/MT/TGF-α (c-Myc–TGF-α) double-transgenic mice has been described elsewhere (22,23). Dysplastic livers were obtained at 4 months from male mice of both transgenics. HCC developed at 8 and 14 months in c-Myc–TGF-α and TGF-α transgenics, respectively. Aminoguanidine (AG) treatment was performed as reported previously (24). In brief, 10 male c-Myc–TGF-α transgenic mice received drinking water containing AG hemisulfate (Sigma Chemical Co., St Louis, MO) at 2000 p.p.m., from the age of 5 weeks, whereas the control group (10 males) received tap water. Animals' water consumption was checked twice a week and remained unaffected by the presence of AG. Treated and untreated animals were killed at 10 months of age, when 100% of untreated c-Myc–TGF-α transgenic mice display HCC (25). Animals received human care, and study protocols were in compliance with National Institutes of Health guidelines for the use of laboratory animals.

Six normal livers and two HCC subclasses of 39 and 46 HCC, characterized by a shorter (<3 years) or longer (>3 years) patients' survival length following liver partial resection, respectively, and corresponding surrounding non-tumor liver tissues were used. All patients selected for the present study died of HCC recurrence, whereas the patients deceased of liver failure were excluded from the study. Patients' clinicopathological features are shown in supplementary Table 1 (available at *Carcinogenesis* Online). Liver tissues were kindly provided by Dr Snorri S.Thorgeirsson (Laboratory of Experimental Carcinogenesis, National Cancer Institute, Bethesda, MD). Institutional Review Board approval was obtained at participating hospitals and the National Institutes of Health.

HuH7 and HepG2 human HCC cell lines were maintained as monolayer cultures in Dulbecco's modified Eagle's medium supplemented with 10% fetal bovine serum. Cell lines were plated at a density of 2.0×10^6 cells in 10 cm dishes and treated with 50, 100 and 200 μM AG (iNOS inhibitor; Cayman Chemical, Ann Arbor, MI) or Glyco-S-nitroso-N-acetyl penicillamine-2 (GS2) (NO• donor), 2 mM sulfasalazine (Sulfa) (IKK inhibitor; EMD Biosciences, San Diego, CA) and 20 mM UO126 (mitogen-activated kinase kinase (MEK) inhibitor; Cell Signaling Technology, Danvers, MA). A total of 2.0×10^3 cells were plated in 96-well plates and grown for 12 h. Subsequently, cells were subjected to serum deprivation for 24 h. iNOS and p65 short interfering RNA (siRNA) experiments were performed as reported (26,27). Transient transfection with either *Ha-Ras* complementary DNA (wild-type) or *Ha-Ras* (dominant-negative mutant, S17N) complementary DNA in a pUSEamp plasmid (Millipore, Billerica, MA) was performed following the manufacturers' protocols.

Histology and immunohistochemistry

Rat and mouse liver tissues were fixed in neutral-buffered paraformaldehyde and processed for hematoxylin and eosin staining, glutathione *S*-transferase, 7–7 isoform, or iNOS immunohistochemistry (5). Number and volume of glutathione *S*-transferase 7–7 isoform-positive liver lesions were calculated by morphometric analysis (5). In mouse samples, tumor size was measured in mm^2 on hematoxylin and eosin-stained sections obtained from the central part of HCC using the ImageJ software as described previously (28).

Proliferation and apoptosis indices

In human and mouse HCC, proliferation and apoptotic indices were determined as reported (29). Cultured cell viability and apoptosis were determined by the WST-1 Cell Proliferation Reagent and the Cell Death Detection Elisa Plus Kit (Roche Diagnostics, Indianapolis, IN), respectively. Apoptosis was induced in HuH7 cells with either 68 μM etoposide plus 10 μM quinidine (inhibiting etoposide efflux by the multidrug resistance protein) for 48 h or 1 μM staurosporine for 4 h as described previously (30).

Evaluation of microvessel density

Human HCCs were stained with mouse monoclonal anti-CD34 antibody (Vector Laboratories, Burlingame, CA) as reported (31). The four highest microvessel density (MVD) areas for each tumor were photographed at high power (×200) and the size of each area was standardized using the ImageJ software. MVD was expressed as the percentage of the total CD34-stained spots per section area (0.94 mm^2).

Quantitative reverse transcription–polymerase chain reaction

Polymerase chain reactions were performed as reported (6). Primers for human and rat iNOS and *RNR-18* genes were chosen with the assistance of the 'Assay-on-Demand™ Products' (Applied Biosystems, Foster City, CA).

Immunoprecipitation

Rat and human tissue samples were processed as reported previously (6). Aliquots of 500 μg of tissue lysates were immunoprecipitated with specific antibodies (supplementary Table 2, available at *Carcinogenesis* Online). Immunoprecipitates were revealed via enhanced chemiluminescence (Santa Cruz Biotechnology, Santa Cruz, CA), and bands were quantified in arbitrary units by the Molecular Imager ChemiDoc XRS, using the Quantity One 1-D Analysis Software, and normalized to β-actin levels.

Electrophoretic mobility shift assay and supershift analysis

Proteins were extracted and electrophoretic mobility shift assay was performed as described (17). Briefly, nuclear extracts were incubated for 30 min with 1 μg of poly(dI-dC) (GE Health Care, Milano, Italy) in binding buffer containing 2 μg of consensus NF-kB probe [consensus binding sites of NF-kB: 5′-AGTTGAGGGGACTTTCCCAGGC (Santa Cruz Biotechnology)] end labeled with [γ-^{32}P]adenosine triphosphate by T4 polynucleotide kinase (Roche Diagnostics). Samples were separated on non-denaturating 4.5% polyacrylamide gel. Dried gels were analyzed by Instant Image Analyzer (Packard Bioscience, Milano, Italy). NF-kB activation in human and mouse liver tissues was determined by the TransAM™ NF-kB p65 kit (Active Motif, Carlsbad, CA) following the manufacturer's protocol.

Determination of Ha-RAS activity

Levels of activated Ha-*RAS* [Ha-*RAS*–guanosine triphosphate (GTP)] bound to v-raf1 murine leukemia viral oncogene homolog 1 were determined using the Ras Activation Assay Kit (Millipore) following the manufacturer's instructions.

Random amplified polymorphic DNA analysis

Twenty-two previously designed primers were used to score genomic alterations in mouse and human HCC, and random amplified polymorphic DNA analysis reaction was performed as described (28). Differences were scored in case of change in the intensity, absence of a band or appearance of a new band in HCC when compared with corresponding non-tumorous livers. The frequency of altered random amplified polymorphic DNA analysis profiles was calculated for each liver lesion as reported (32).

Statistical analysis

Student's *t*-test and Tuckey–Kramer test were used to evaluate statistical significance. Fisher's exact test was used for comparative analysis of the survival of HCC patient subgroups. Multiple regression analysis was performed to calculate correlation coefficient (R) using GraphPad InStat 3 (http://www.graphpad.com). Values of $P < 0.05$ were considered significant. Data are expressed as means ± SDs.

Results

Development of rat neoplastic liver lesions

Four and six weeks after initiation of F344 and BN rats with diethylnitrosamine, glutathione *S*-transferase 7-7(+) foci of altered hepatocytes developed, occupying 40–58% of the liver without interstrain differences, in agreement with previous reports (6). Further evolution of foci to early nodules was more pronounced in F344 than BN rats, and at 12 weeks, clear/eosinophilic cell nodules occupied 94 ± 5.6 and 49 ± 2.1% of liver in F344 and BN rats, respectively ($P < 0.0001$, $n = 10$). Dysplastic nodules/well-differentiated HCCs and moderately/poorly differentiated HCCs were present at 32 and 57 weeks in F344 rats. Different from F344 liver lesions, nodules of BN rats did not show atypical features and consisted only of clear/eosinophilic cells. Well-differentiated/moderately differentiated HCC developed in BN rats at 60 weeks.

Genetic susceptibility influences iNos expression and NF-kB and Ha-Ras activity in rat lesion

Progressive rise in i*Nos* messenger RNA (mRNA) and protein levels occurred in F344 and BN preneoplastic liver, 4–12 weeks after initiation, with respect to normal control, without major interstrain differences (Figure 1). iNos remained almost unchanged in nodules and HCCs of BN rats, whereas a sharp and progressive upregulation

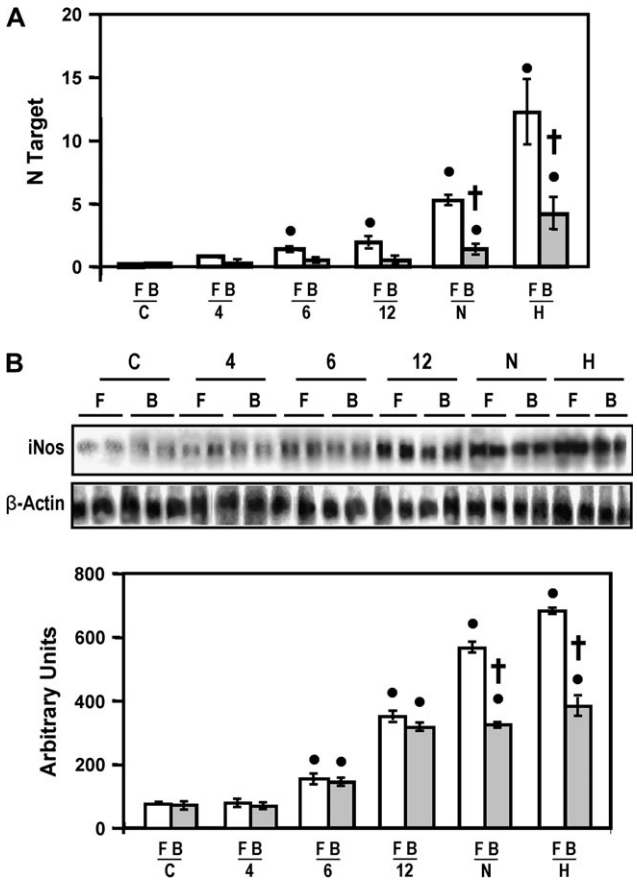

Fig. 1. Expression of *iNos* mRNA and protein during rat liver carcinogenesis in F344 (F, white columns) and BN (B, gray columns) rats. Preneoplastic liver (4–6 weeks after initiation), early nodules (12 weeks), dysplastic nodules (N, 32 weeks) and HCC (H, 56–60 weeks) were induced by the resistant hepatocyte protocol. (**A**) *iNos* mRNA levels were determined by quantitative reverse transcription–polymerase chain reaction. N Target = $2^{-\Delta Ct} \times 10^3$; ΔCt = CtRNR-18 − Ct target gene. Data are means ± SDs of N target of at least five rats for control (C), preneoplastic liver and neoplastic lesions. Tuckey–Kramer test: dot refers to carcinogen treated versus control, $P < 0.001$; dagger refers to BN versus F344, $P < 0.001$. (**B**) Upper panel: representative immunoprecipitation analysis of iNos in preneoplastic and neoplastic rat liver. Protein lysates were immunoprecipitated with specific antibodies and separated by sodium dodecyl sulfate–polyacrylamide gel electrophoresis. Lower panel: chemiluminescence analysis showing mean ± SD of at least five rats for liver lesions. Optical densities of the peaks were normalized to β-actin values and expressed in arbitrary units. Tuckey–Kramer test: dot refers to carcinogen-treated versus control, at least $P < 0.01$; dagger refers to BN versus F344, at least $P < 0.001$.

occurred in corresponding lesions from F344 rats. iNos immunoreactivity was limited to preneoplastic and neoplastic lesions of both F344 and BN rats (supplementary Figure S1, available at *Carcinogenesis* Online). In agreement with immunoprecipitation data, no interstrain differences in iNos immunolabeling were found at 4 and 12 weeks, whereas lower density and/or extension of iNOS immunoreactivity were detected in 32 weeks nodules and HCC of BN than in corresponding F344 rat lesions.

To assess the effect of iNos upregulation on Ikk/NF-kB and Ras/Erk cascades, iNos interconnections with these pathways were evaluated in dysplastic nodules and HCC of F344 and BN rats. In nodules and HCCs of F344 rats, marked iNos induction was paralleled by increases in Ikk-α/β, nuclear and phosphorylated p65 and NF-kB target gene, Bcl-xL (Figure 2A and supplementary Figure S2A, available at *Carcinogenesis* Online). Furthermore, decrease in inhibitor of kB (Ikb)-α was coupled to the rise in its ubiquitinated form. In BN rat lesions, small increase in iNos expression was associated with no change in Ikk-α/β level, slight decrease in IkB-α and small changes in ubiquitinated IkB-α. In addition, increases in total and activated Ha-Ras (Ha-Ras-GTP) occurred in nodules and HCCs of F344 rats, whereas significantly lower increases or no increase occurred in corresponding BN rat lesions.

Low NF-kB activation in BN rat lesions was confirmed by relatively low increase in nuclear and phosphorylated p65 and Bcl-xL (Figure 2A and supplementary Figure S2A, available at *Carcinogenesis* Online) and by interstrain differences in NF-kB binding to DNA (supplementary Figure S3, available at *Carcinogenesis* Online). Binding activity progressively increased from nodules to HCCs of both strains, but always at higher levels in F344 rat lesions.

iNos signaling in TGF-α and c-Myc–TGF-α transgenic mice

iNos interplay with Ikk/NF-kB and Ras/Erk signaling evaluation in transgenic mice (Figure 2B and supplementary Figure S2B, available at *Carcinogenesis* Online) showed progressive iNos protein upregulation from dysplastic liver to HCC, with highest values in c-Myc–TGF-α double transgenics. Very low increase in Ha-Ras levels occurred, whereas progressive rises from dysplastic liver to HCC, with highest values in double-transgenic mice, occurred for Ha-Ras-GTP, pErk1/2, Ikk-α/β, nP65 and the complex E2f1–Dp1. Increase in phosphorylated pRb also occurred in dysplastic and neoplastic liver of both transgenic mice (with highest levels in double transgenics), whereas decreased Ikb-α expression was detected in dysplastic and neoplastic lesions of both transgenic mice. NF-kB activation in dysplastic and neoplastic lesions of transgenic mice underwent remarkable and progressive increase from dysplastic to neoplastic liver with highest values in c-Myc–TGF-α transgenics (supplementary Figure S4A, available at *Carcinogenesis* Online).

iNOS signaling correlates with growth of human liver and patients' survival

The results from rodent models suggest a relationship between iNOS signaling and liver lesions propensity to progress. Thus, we tested this possibility in human HCC from patients with different survival rates (Figure 2C and supplementary Figure S2C, available at *Carcinogenesis* Online). Upregulation of iNOS, total and activated Ha-RAS, IKK-α/β, total and nuclear P65, BCL-xL, phosphorylated PRb and E2F1–DP1 complexes and decrease in IKB-α occurred in all human HCCs when compared with normal liver and was highest in HCCP. Lower but significant increases occurred in surrounding liver (SL) without differences linked to HCC subtype. These changes were associated with a sharp and progressive increase in NF-kB activation in SL and HCCs, with the highest values in HCCP (supplementary Figure S4b, available at *Carcinogenesis* Online). In HCC, *iNOS* mRNA levels were 1.8-fold higher in HCCP than HCCB (N target $\times 10^3$: 2.32 ± 1 and 1.23 ± 0.4, means ± SDs; $n = 46$ and 39 for HCCP and HCCB, respectively, $P < 0.0001$). Similarly, iNOS protein levels were 3-fold higher in HCCP than in HCCB (arbitrary units: 473.43 ± 158.62 and 150.53 ± 40.4; $n = 46$ and 39, $P < 0.0001$). Moreover, ∼2-fold higher proliferation index and MVD and ∼3-fold lower apoptotic index occurred in HCCP than HCCB (supplementary Table 1, available at *Carcinogenesis* Online). Since these parameters, similar to gene expression data, are linked to HCC prognosis, we evaluated their correlation with i*NOS* expression (Figure 3). iNOS protein levels positively correlated with proliferation index, MVD and genomic instability and negatively with apoptotic index and patients' survival. No other clinicopathological parameters, including patients' age, presence of cirrhosis, tumor size and grade and serum α-fetoprotein levels, were correlated with proliferation and apoptotic indices, MVD and survival length. However, survival length was inversely correlated with the proliferation index ($r^2 = 0.5862$, $P < 0.0001$) and directly correlated with the apoptosis index ($r^2 = 0.5277$, $P < 0.0001$).

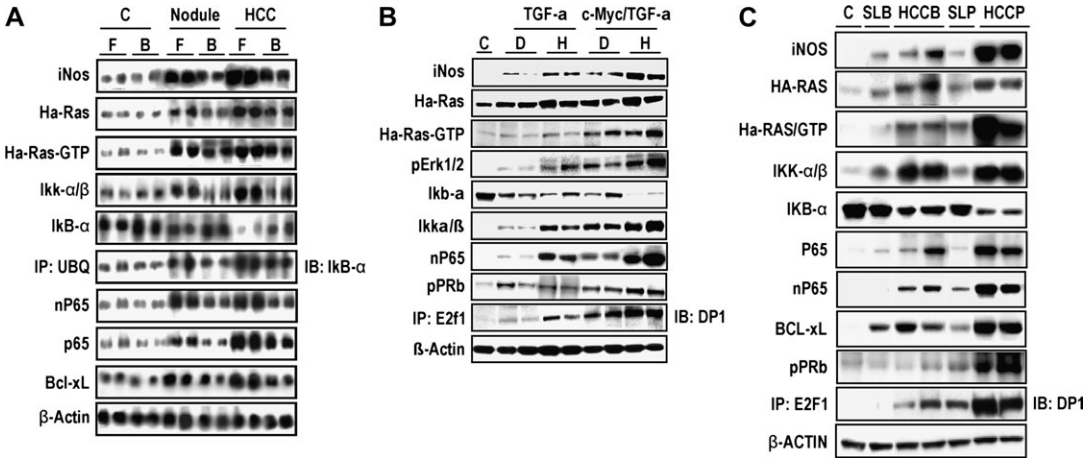

Fig. 2. Representative immunoprecipitation analysis of the expression of iNos and members of the IKK–NF-kB and Ha-RAS/ERK cascades in preneoplastic and neoplastic lesions of F344 and BN rats, TGF-α and c-Myc–TGF-α transgenic mice and human HCC. (**A**) Dysplastic nodules (32 weeks after initiation) and HCCs (56–60 weeks) were induced in rats by the resistant hepatocyte protocol. (**B**) Dysplastic liver was collected at 4 months from both TGF-α and c-Myc–TGF-α transgenics; HCCs were collected at 8 and 14 months from c-Myc–TGF-α and TGF-α transgenics, respectively. (**C**) SL and HCC subtypes with better and poorer prognosis were collected from patients with >3 and <3 years survival length, after partial liver resection, respectively (see supplementary Table 1, available at *Carcinogenesis* Online). Protein lysates were immunoprecipitated with specific antibodies and separated by sodium dodecyl sulfate–polyacrylamide gel electrophoresis. Ubiquitinated Ikb-α was determined through immunoprecipitation with anti-ubiquitin antibody and probing the membranes with the anti-Ikb-α antibody. The E2F1–DP1 complexes were determined through immunoprecipitation with the anti-E2F1 antibody and probing the membranes with the anti-DP1 antibody. Abbreviations: C, control (normal liver); F and B, F344 and BN rats, respectively; D and H, dysplastic liver and HCC, respectively; SLB/HCCB and SLP/HCCP, human SL/HCC with better and poorer prognosis, respectively.

Manipulation of iNOS production influences proliferation of HCC cells in vitro

Above results suggest a role for iNOS expression and NO• production in deregulation of HCC growth. To test this hypothesis, we evaluated the effect of an iNOS inhibitor, AG (24), and a NO• producer, GS2, on the growth rate of HuH7 and HepG2 human HCC cell lines. A significant dose-dependent inhibition of cell proliferation by AG and an enhancing effect of NO• production were obtained (Figure 4). These effects were enhanced when apoptosis inducers such as etoposide (Figure 4 insets) or staurosporine (data not presented) were added to the culture medium. Furthermore, AG administration to c-Myc–TGF-α transgenic mice induced 5-, 2.8- and 1.9-fold decreases in iNos protein expression, genomic instability and proliferation rate of HCC, respectively, and a 15-fold rise in apoptotic index (Figure 5). This was associated with a 3.5- and 1.8-fold reduction in HCC yield per mouse and tumor size, respectively, as well as with ∼2-fold decrease in expression of growth-related genes such as active Ha-Ras-GTP, pErk1/2, np65 and phosphorylated pRb. The sharp increase in apoptosis following iNOS inhibition was associated to decrease in the levels of antiapoptotic proteins Bcl-xL, Xiap and ciap1 and a rise in the proapoptotic pJnk.

Analysis of iNOS cross talk with IKK/NF-kB and Ha-RAS/ERK cascades

Next, we examined the interactions of iNOS/IKK/NF-kB and iNOS/Ha-RAS/ERK axes by manipulating NO• production and inhibiting some key steps in NF-kB and ERK synthesis, such as IKK-α/β and MEK, respectively, in the same HCC cell lines (Figure 6 and supplementary Figures S5 and S6, available at *Carcinogenesis* Online). iNOS inhibition by AG (Figure 6A and supplementary Figure S5A, available at *Carcinogenesis* Online) resulted in 50–65% decrease in IKK, free P65 and BCL-xL, phosphorylated PRb, XIAP and cIAP1 and rise in IKB-α expression and P65–IKB-α immunocomplexes and pJNK. A decline in total and Ha-RAS-GTP also occurred, but only at the highest AG concentration. Similar results were obtained with siRNA against iNOS, which also inhibited pERK1/2 (Figure 6B and supplementary Figure S5B, available at *Carcinogenesis* Online). In contrast, stimulation of NO• production by GS2 (Figure 6C and supplementary Figure S5C, available at *Carcinogenesis* Online) increased Ha-RAS activation, without changing Ha-RAS total levels, and pERK1/2 expression. This was paralleled by 50% reduction in IKB-α levels, marked upregulation of total and nuclear P65, phosphorylated PRb, rise in antiapoptotic proteins and decrease in pJNK. Opposite results were found when HCC cells were treated with the IKK inhibitor Sulfa (23): ∼250% rise in IKB-α and 60–70% decrease in total and nuclear P65 occurred (Figure 6D and supplementary Figure S5D, available at *Carcinogenesis* Online). This was associated with iNOS downregulation, which confirms iNOS gene targeting by active NF-kB (33) and inhibition of the Ha-RAS/ERK signaling, as shown by decrease in Ha-RAS-GTP and pERK1/2 levels. Finally, NF-kB inhibition by siRNA (Figure 6E and supplementary Figure S5E, available at *Carcinogenesis* Online) induced a fall in iNOS, Ha-RAS-GTP and pERK1/2 expression.

Activation of RAS/ERK signaling by transient *Ha-RAS* transfection promoted sharp Ha-RAS and pERK1/2 upregulation, associated with 120 and 30% rise in iNOS and NF-kB expression, respectively, whereas the same genes were downregulated following transient transfection with dominant-negative mutated *Ha-Ras* (Figure 6F and G and supplementary Figure S6A and B, available at *Carcinogenesis* Online). Similarly, suppression of the Ha-RAS/pERK1/2 signaling by the MEK inhibitor UO126 (34) triggered a strong decrease in pERK1/2 associated with a 37–70% decrease in iNOS expression (Figure 6H and supplementary Figure S6C, available at *Carcinogenesis* Online), supporting iNOS targeting by pERK1/2, and rise in IKB-α paralleled by decrease in P65 expression.

Role of cytokines

To verify the role of inflammatory cytokines, which are known to be involved in iNOS activation (11), we determined the expression of interleukin (IL)-1B, IL-6, tumor necrosis factor-α (TNF-α) and interferon-γ (IFN-γ) in human and mice liver lesions (supplementary Figure S7, available at *Carcinogenesis* Online). Cytokine mRNA levels underwent sharp increases in dysplastic and neoplastic liver of both TGF-α and c-Myc–TGF-α transgenics when compared with normal liver ($P < 0.0001$). In general, cytokine expression was higher in HCC than dysplastic liver, but this difference reached the level of significance only in TGF-α transgenics, for IL-1B, and in c-Myc–TGF-α transgenics, for other cytokines. TNF-α and IFN-γ levels were 1.6-fold

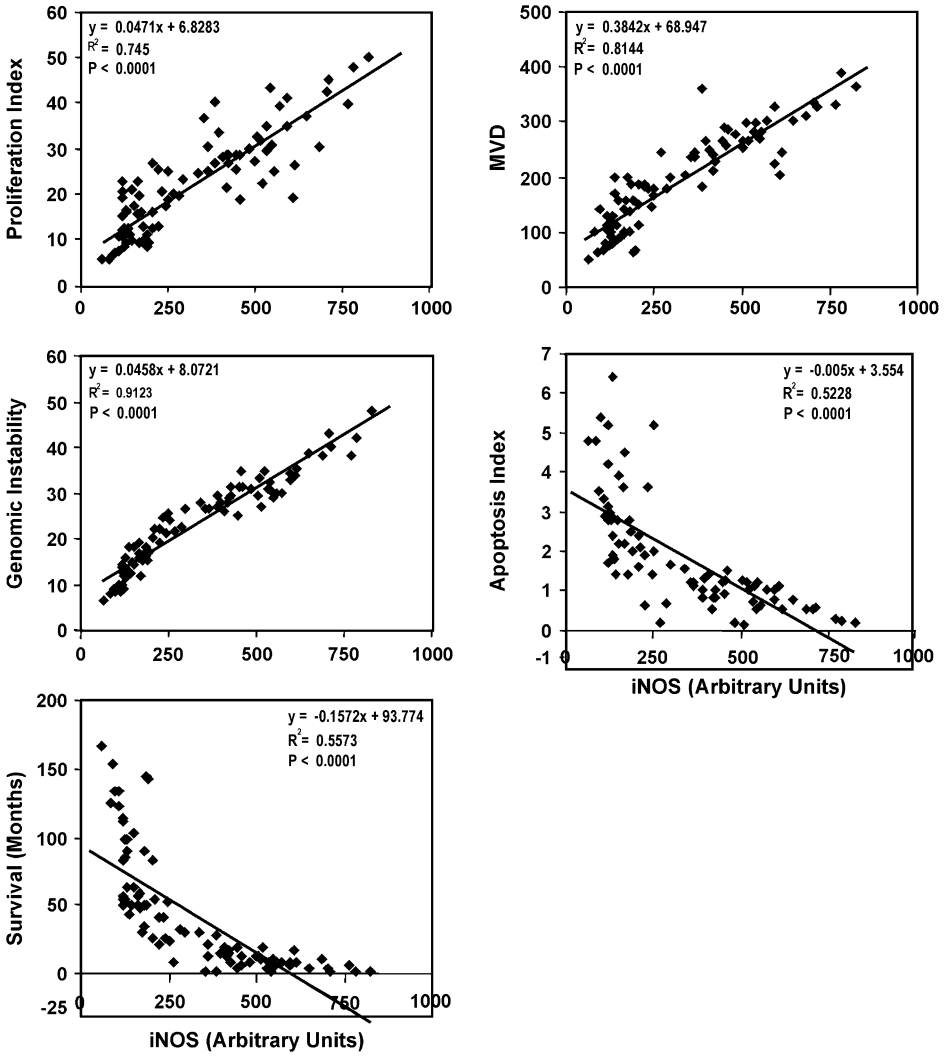

Fig. 3. Correlation of iNOS protein levels with proliferation index, MVD, genomic instability, apoptosis index and patients' survival in 39 human HCCB and 46 HCCP. Proliferation and apoptotic indices were determined in human HCC by counting Ki-67-positive cells and apoptotic figures and expressed as percentage of total hepatocytes. MVD was determined by counting cells stained with anti-CD34 antibody. Genomic instability represents the percentage of DNA alterations as evaluated by random amplified polymorphic DNA analysis.

higher in HCC of TGF-α than c-Myc–TGF-α transgenics. IL-1B, IL-6 and TNF-α increased in human SL and HCC, reaching highest values in HCCP. Increase in IFN-γ also occurred in human lesions when compared with normal livers, but higher values were found in surrounding non-tumorous liver than in HCC.

Discussion

Our results assign a role to iNOS upregulation in the control of the proliferative phenotype of preneoplastic and neoplastic liver cells through the activation of the IKK/NF-kB axis (supplementary Figure S8, available at *Carcinogenesis* Online). This is shown by (i) the association of marked iNos overexpression with Ikk and NF-kB upregulation and Ikb-α downregulation in HCC from F344 rats and c-Myc–TGF-α double-transgenic mice, susceptible to hepatocarcinogenesis, and human HCC; (ii) the association of the inhibition of iNos activity by AG in double transgenics *in vivo* with growth restraint, increase in apoptosis and fall in tumor yield and inhibition of Ikk/NF-kB signaling; (iii) the observation that *in vitro* inhibition of iNOS activity by AG or siRNA results in increased IKB-α, decreased IKK expression, NF-kB activation, phosphorylated (inactive) pRb and cell growth, whereas the opposite occurs with the NO• producer, GS2, and (iv) the association of IKK inhibition by Sulfa and consequent rise in IKB-α and decrease in NF-kB with iNOS fall, in agreement with a role of NF-kB in the control of iNOS expression (33).

Our results also imply a cross talk between iNOS and Ha-RAS/ERK in rat, mouse and human HCC. Indeed, iNOS upregulation in these lesions is associated with increase in active Ha-RAS. NO• overproduction, induced by elevated oxidative stress in c-Myc–TGF-α transgenic mice (18) and by GS2 in HCC cell lines, triggers Ha-RAS and ERK upregulation, whereas iNOS inhibition by AG or siRNA is associated with decreased Ha-RAS activation. Furthermore, Ha-RAS and pERK1/2 overexpression in HCC cell lines transfected with Ha-*Ras* is associated with iNOS and NF-kB upregulation, whereas inhibition of pERK1/2 activation by UO126 (34) or transfection of the dominant-negative mutant Ha-*Ras* downregulates iNOS and strongly reduces NF-kB activation. These observations implicate a role of the activation of Ha-RAS/ERK signaling by iNOS in the regulation of NF-kB activity. Conversely, the inhibition of IKK/NF-kB axis by Sulfa or p65 siRNA results in a great iNOS fall, suggestive of iNOS expression regulation by the IKK/NF-kB axis. This agrees with recent evidence indicating a role of active ERK, mediated by NF-kB, on bacterial lipopolysaccharide-induced iNOS expression in RAW264.7 cells (35). In addition, dominant-negative mutant of

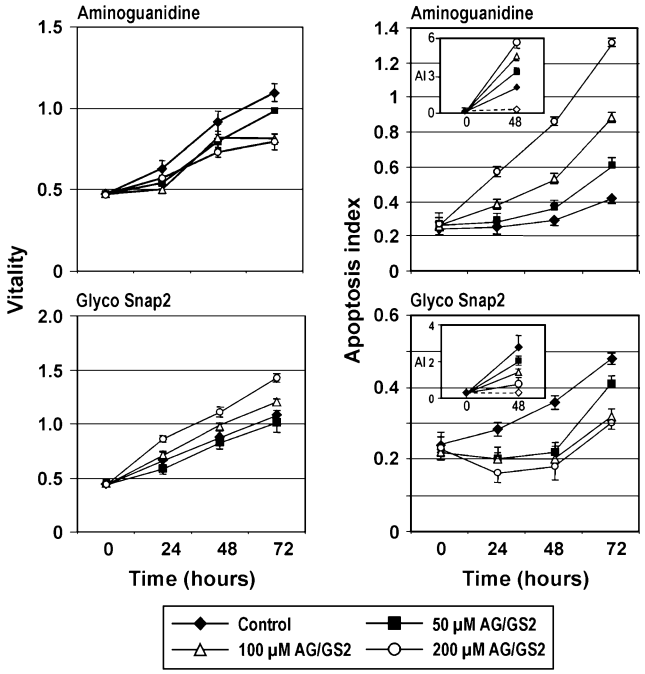

Fig. 4. Effect of AG and GS2 on *in vitro* growth and apoptosis of human HCC cells. HuH7 cells were cultured for the times indicated in the presence of 0–200 μM AG or GS2. Insets: the effects of AG and GS2 were tested on HuH7 cells, whose apoptosis was induced by etoposide plus quinidine (inhibiting etoposide efflux by the multidrug resistance protein). Dotted line refers to untreated cell without etoposide. Data are means of three different cultures. Tuckey–Kramer test: 50 μM, $P < 0.001$ at 48 and 72 h; 100 and 200 μM, $P < 0.001$ at 24–72 h. Equivalent results obtained in HepG2 cells are not shown. Insets: 48 h, AG/GS2 at all concentrations versus controls (etoposide alone), at least $P < 0.05$.

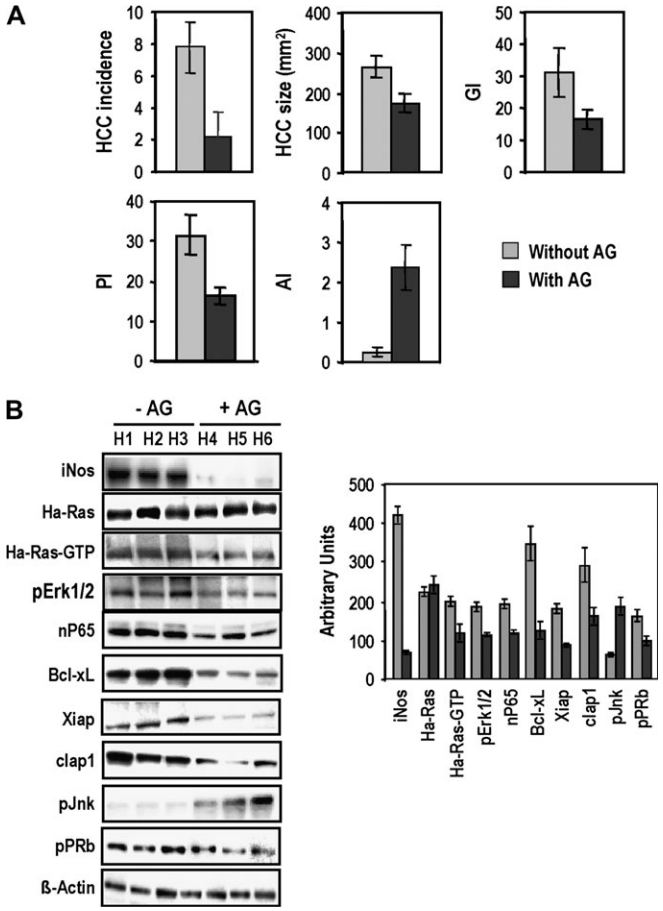

Fig. 5. Effect of AG on development and phenotypic and genotypic changes of HCC in c-Myc–TGF-α transgenic mice. (**A**) Ten c-Myc–TGF-α transgenic mice received drinking water containing AG hemisulfate at 1500 p.p.m., from the age of 5 weeks up to killing (10 months). The control group ($n = 10$) received instead tap water. (A) HCC incidence (number of tumors per mice), HCC size (in mm^2), genomic instability (GI, percentage of DNA alterations as evaluated by random amplified polymorphic DNA analysis) and proliferation and apoptosis indices (PI and AI, percentage of Ki-67-positive cells and apoptotic figures in HCCs) were expressed as means ± SDs. Tuckey–Kramer test: AG versus control, at least $P < 0.001$. (**B**) Representative immunoprecipitation analysis (left) of the expression of iNos and members of the IKK–NF-kB and Ha-RAS/ERK pathways. Protein lysates were immunoprecipitated with specific antibodies and separated by sodium dodecyl sulfate–polyacrylamide gel electrophoresis. Right: chemiluminescence analysis showing mean ± SD. Optical densities of the peaks were normalized to β-actin values and expressed in arbitrary units. Tuckey–Kramer test: AG versus control. At least $P < 0.001$ for all genes, except for Ha-Ras protein level that was not affected by AG.

$p21^{RAS}$ inhibits both iNOS induction by bacterial lipopolysaccharide and NF-kB activation in primary astrocytes (36). The mechanism of NF-kB regulation by pERK1/2 is not fully understood. Recent observations show that pERK1/2 activates Aurora-A, which in turn may activate NF-kB through IKB-α inhibition (37). The possibility that pERK1/2 contributes to NF-kB upregulation via direct activation of iNOS may also be taken into account (14), but requires experimental support.

Our results substantiate a clear antiapoptotic effect of NO• production in our experimental conditions. Indeed, iNOS inhibition by AG resulted in sharp increase in apoptosis in c-Myc–TGF-α transgenics and HCC cell lines, whereas NO• production by GS2 inhibited apoptosis of *in vitro* growing HCC cells, both in basal conditions and in the presence of either etoposide or staurosporine, two apoptosis inducers. In transgenic mice and human HCC cell lines, iNOS antiapoptotic effect seems to be mediated by the NF-kB cascade. The latter induces various antiapoptotic proteins, such as BCL-xL, XIAP and cIAP1, and inhibits the proapoptotic pJNK (33). Accordingly, iNOS suppression by AG triggered downregulation of NF-kB and antiapoptotic proteins and upregulation of pJNK, in c-Myc–TGF-α and human HCC cell lines. However, the present findings cannot exclude the contribution of other mechanisms to the antiapoptotic action of iNOS.

Upregulation of iNOS and its downstream targets are highest in HCCs prone to progression as those of susceptible F344 rats and c-Myc–TGF-α transgenic mice and in human HCCP. Furthermore, iNOS levels are positively correlated with genomic instability, proliferation rate and MVD of HCC and negatively correlated with apoptosis and patients' survival. This body of evidence suggests that iNOS upregulation and changes in iNOS/NF-kB and iNOS/Ha-RAS/ERK cross talks are prognostic markers for HCC. Previous studies on the prognostic value of iNOS were often contradictory and only few of them regarded human HCC. An association of iNOS overexpression with poor prognosis has been found for gastric cancer (38), adenoid cystic carcinoma of salivary glands (39), fibrous histiocytoma (40) and colorectal cancer (41) and seems to be mediated by its angiogenic properties and intensified by cyclooxygenase 2 upregulation (41,42). However, no correlation of iNOS overexpression with prognosis (43,44) or even its protective effect through induction of apoptosis (45,46) has been reported for various tumors. In HCC, a significant association of iNOS and metalloproteinase-9 expression with HCC recurrence has been described (19). This apparently contrasts with the absence of significant differences in the proliferation and apoptosis indices in two human HCC subpopulations distinguished on the basis of the presence or absence of the iNOS transcript as determined by semiquantitative reverse transcription–polymerase

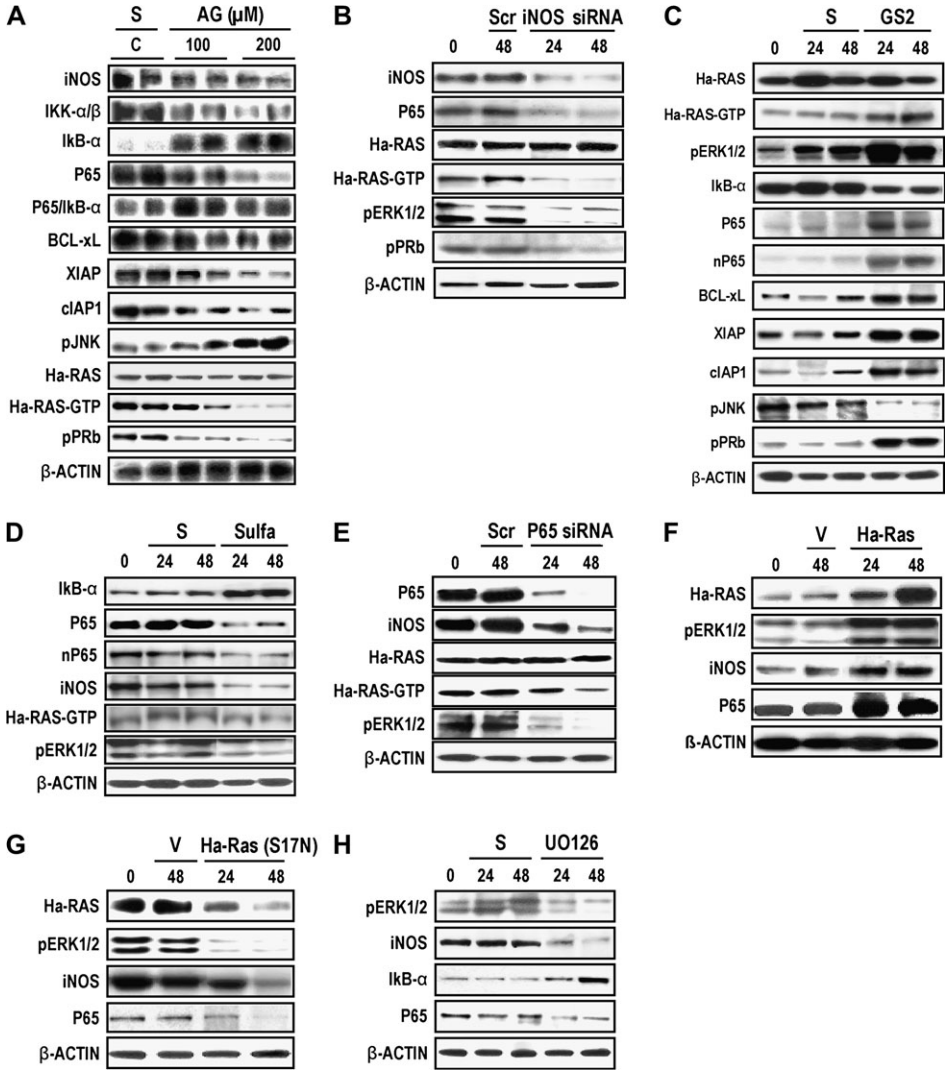

Fig. 6. Representative immunoprecipitation blots showing the effect of AG, GS2, Sulfa, UO126 and siRNAs against iNOS and P65 and transfection of active Ha-*Ras* (Ha-Ras) and dominant-negative mutated Ha-*Ras* (Ha-Ras S17N) on gene expression in HuH7 cell line. (**A**) Cells grown 48 h in the presence of AG and controls contained solvent (S) alone. (**B** and **E**) Cells grown 24 and 48 h in the presence of siRNA against iNOS and P65, respectively, or grown 48 h with scramble (Scr) oligonucelotides. (**C**, **D** and **H**) Cultures grown 24 and 48 h in the presence of 200 μM GS2, Sulfa and UO126, respectively, or solvent alone. Untreated control at 0 time (0). (**F** and **G**) Transient transfection of HuH7 cells was performed with *Ha-Ras* complementary DNA (wild-type) or *Ha-Ras* (dominant-negative mutant, S17N) complementary DNA, respectively, in a pUSEamp plasmid. Cells were harvested 48 h after transfection. Controls are not transfected cells (0) and cells transfected with vector alone (V). Equivalent results obtained in HepG2 cells are not shown. Protein lysates were immunoprecipitated with specific antibodies and separated by sodium dodecyl sulfate–polyacrylamide gel electrophoresis.

chain reaction (20). However, we found, by highly sensitive quantitative reverse transcription–polymerase chain reaction, *iNOS* mRNA expression in human normal liver and all HCCs, with highest values in HCCP. These results were confirmed at iNOS protein level, which was positively correlated with the proliferation index and negatively correlated with the apoptotic index. Presumably, the discrepant results may either depend on the heterogeneity of the two subgroups examined in the previous research (20), as shown by the high variability of proliferation and apoptosis indices in those HCC subgroups, or on the sensitivity of the method used to detect iNOS levels. Another observation apparently arguing against a prominent role of iNos in hepatocarcinogenesis is that i*Nos* gene ablation does not prevent HCC development in mice fed a choline-deficient, L-amino acid-deficient diet (47). Delayed liver regeneration occurring in *iNos* knockout mice was attributed to the absence of NO• protection against cytokine-induced liver steatosis, necrosis and apoptosis (48). However, in the methyl-deficient model of hepatocarcinogenesis, high production of lipid peroxides in hepatocyte nuclei occurs (49). This, in addition to massive liver injury, may cause DNA damage and genomic instability in an iNos-independent manner. Selective growth of initiated cells, resistant to oxidative damage (49), favors their evolution to cancer.

Another important aspect of our results is the demonstration that *iNos*-linked signaling in liver preneoplastic and neoplastic lesions is largely influenced by the susceptibility to hepatocarcinogenesis either dependent on susceptibility genes or genomic engineering. The resistant phenotype is characterized by the incapacity of early preneoplastic lesions to acquire autonomous growth (5), resulting in a low capacity of preneoplastic lesions to progress to HCC. Autonomous growth of the lesions is supported, in susceptible rats, by marked deregulation of the cell cycle (5,6) and Ras/Erk pathway (50). These alterations are limited or absent in the lesions of resistant rats (5,6). In this report, we found iNos upregulation in very early stages of hepatocarcinogenesis in both F344 and BN rats. However, after the sixth week, when a high number of autonomously growing nodules appear in the liver of F344 rats (6), iNos protein expression sharply and progressively increased in nodules and HCC. Much lower changes

occurred in slow-growing nodules and HCC of BN rats. A link between fast growth and signaling deregulation characterizes human HCCP, whereas the behavior of HCCB is more similar to that of the lesions of resistant rats (5,6). This does not necessarily imply a genetic regulation of signaling pathways in humans like that found in rodents, in which polygenic inheritance with several low-penetrance genes and a main gene regulates the genetic predisposition to HCC (4). Even if a genetic model, similar to that of rodents, can influence human hepatocarcinogenesis (51), further studies are needed to clarify the influence of susceptibility genes on signaling pathways supporting tumor growth and progression in humans.

In conclusion, we demonstrate that iNOS overexpression contributes to growth deregulation in preneoplastic and neoplastic liver cells through NF-kB activation and show for the first time the existence of a cross talk between Ha-Ras/ERK and iNOS/IKK/NF-kB axis in these lesions. This does not exclude *per se* the activation of iNOS signaling by other mechanisms, such as inflammatory cytokines (11) or the Wnt/β-catenin signaling (52). Indeed, IL-1B, IL-6, TNF-α and IFN-γ expressions increase in dysplastic and neoplastic liver of transgenic mice, with highest values for TNF-α and IFN-γ, in double-transgenic HCC. Rise in cytokine expression also occurs in human HCC and SL, with highest values in HCCP, for IL-1B, IL-6 and TNF-α. The role of Wnt/β-catenin signaling in iNOS upregulation seems to be unlikely, in our experimental conditions, due to the observation of β-catenin activation (nuclear localization) in ∼30% of HCCs from both F344 and BN rats (M.Frau, unpublished data) expressing sharply different iNos mRNA levels. β-Catenin activation also occurs in a lower percentage of HCC from c-Myc–TGF-α than TGF-α transgenics (12 versus 30%) (28), although highest iNOS expression was found in HCC from double-transgenic mice. Similarly, β-catenin activation was most frequent in human HCCB than HCCP (35 versus 10%; D.F.Calvisi, unpublished data), although HCCB exhibited lower levels of iNOS expression. These data, together with the finding of lack of transcriptional induction of Wnt/β-catenin canonical targets (c-Myc, cyclin D1) in livers displaying an activated form of β-catenin (53), suggest that β-catenin targets might be different depending on the tissue and/or the model examined.

Our results strongly suggest a potential prognostic role of iNOS signaling that should be tested by a large-scale clinical research. The association of the block of iNOS signaling by a specific inhibitor such as AG with a consistent decrease in HCC growth and increase in apoptosis *in vitro* indicates that the key component of this pathway could represent therapeutic targets that, in association with other targets, may contribute to create networked biological therapies (54). Thus, determination of iNOS immunoreactivity status can be proposed as a promising candidate for the identification of high-risk patients who may benefit from the new anticancer drugs targeting iNOS and its interplay with IKK/NF-kB and Ha-RAS/ERK signaling.

Supplementary material

supplementary Figures S1–S8 and Tables 1 and 2 can be found at http://carcin.oxfordjournals.org/

Funding

Associazione Italiana Ricerche sul Cancro and Ministero Università e Ricerca (PRIN).

Acknowledgements

Conflict of Interest Statement: None declared.

References

1. Bosch,F.X. *et al*. (2004) Primary liver cancer: worldwide incidence and trends. *Gastroenterology*, **127**, S5–S16.
2. Bruix,J. *et al*. (2004) Focus on hepatocellular carcinoma. *Cancer Cell*, **5**, 215–219.
3. Feo,F. *et al*. (2000) Genetic alterations in liver carcinogenesis. *Crit. Rev. Oncog.*, **11**, 19–62.
4. Feo,F. *et al*. (2006) Hepatocellular carcinoma as a complex polygenic disease. Interpretive analysis of recent developments on genetic predisposition. *Biochim Biophys Acta Cancer Rev.*, **176**, 126–147.
5. Pascale,R.M. *et al*. (2002) Cell cycle deregulation in liver lesions of rats with and without genetic predisposition to hepatocarcinogenesis. *Hepatology*, **35**, 1341–1350.
6. Pascale,R.M. *et al*. (2005) Role of HSP90, CDC37 and CRM1 as modulators of $P16^{INK4A}$ activity in rat liver carcinogenesis and human liver cancer. *Hepatology*, **42**, 1310–1319.
7. Calvisi,D.F. *et al*. (2005) Molecular mechanisms of hepatocarcinogenesis in transgenic mouse models of liver cancer. *Toxicol. Pathol.*, **33**, 181–184.
8. Lee,J.S. *et al*. (2004) Application of comparative functional genomics to identify best-fit mouse models to study human cancer. *Nat. Genet.*, **36**, 1306–1311.
9. Ying,L. *et al*. (2007) Nitric oxide inactivates the retinoblastoma pathway in chronic inflammation. *Cancer Res.*, **67**, 9286–9293.
10. Lasagna,N. *et al*. (2006) Hepatocyte growth factor and inducible nitric oxide synthase are involved in multidrug resistance-induced angiogenesis in hepatocellular carcinoma cell lines. *Cancer Res.*, **66**, 2673–2682.
11. Hussain,S.P. *et al*. (2007) Inflammation and cancer: an ancient link with novel potentials. *Int. J. Cancer*, **121**, 2373–2380.
12. Zingarelli,B. *et al*. (2002) Absence of inducible nitric oxide synthase modulates early reperfusion-induced NF-kB and AP-1 activation and enhances myocardial damage. *FASEB J.*, **16**, 327–342.
13. Deora,A.A. *et al*. (2000) Recruitment and activation of Raf-1 kinase by nitric oxide-activated Ras. *Biochemistry*, **39**, 9901–9908.
14. Ellerhorst,J.A. *et al*. (2006) Regulation of iNOS by the p44/42 mitogen-activated protein kinase pathway in human melanoma. *Oncogene*, **25**, 3956–3962.
15. Zhao,Q. *et al*. (1999) Mitogen-activated protein kinase/ERK kinase kinases 2 and 3 activate nuclear factor-kappaB through IkB kinase-alpha and IkB kinase-beta. *J. Biol. Chem.*, **274**, 8355–8358.
16. Moriyama,A. *et al*. (1997) High plasma concentrations of nitrite/nitrate in patients with hepatocellular carcinoma. *Am. J. Gastroenterol.*, **92**, 1520–1523.
17. Simile,M.M. *et al*. (2005) Chemopreventive *N*-(4-hydroxyphenyl)retinamide (fenretinide) targets deregulated NF-kB and Mat1A genes in the early stages of rat liver carcinogenesis. *Carcinogenesis*, **26**, 417–427.
18. Calvisi,D.F. *et al*. (2004) Vitamin E down-modulates iNOS and NADPH oxidase in c-Myc/TGF-alpha transgenic mouse model of liver cancer. *J. Hepatol.*, **41**, 815–822.
19. Sun,M.H. *et al*. (2005) Expressions of inducible nitric oxide synthase and matrix metalloproteinase-9 and their effects on angiogenesis and progression of hepatocellular carcinoma. *World. J. Gastroenterol.*, **11**, 5931–5937.
20. Ikeguchi,M. *et al*. (2002) Inducible nitric oxide synthase and survivin messenger RNA expression in hepatocellular carcinoma. *Clin. Cancer Res.*, **8**, 3131–3136.
21. Solt,D.B. *et al*. (1997) Rapid emergence of carcinogen-induced hyperplastic lesions in a new model for the sequential analysis of liver carcinogenesis. *Am. J. Pathol.*, **88**, 595–618.
22. Lee,G.H. *et al*. (1992) Development of liver tumors in transforming growth factor alpha transgenic mice. *Cancer Res.*, **52**, 5162–5170.
23. Weber,C.K. *et al*. (2000) Suppression of NF-kappaB activity by sulfasalazine is mediated by direct inhibition of IkappaB kinases alpha and beta. *Gastroenterology*, **119**, 1209–1218.
24. Misko,T.P. *et al*. (1993) Selective inhibition of the inducible nitric oxide synthase by aminoguanidine. *Eur. J. Pharmacol.*, **233**, 119–125.
25. Murakami,H. *et al*. (1993) Transgenic mouse model for synergistic effects of nuclear oncogenes and growth factors in tumorigenesis: interaction of c-Myc and transforming growth factor alpha in hepatic oncogenesis. *Cancer Res.*, **53**, 1719–1723.
26. Machida,K. *et al*. (2004) Hepatitis C virus infection activates the immunologic (type II) isoform of nitric oxide synthase and thereby enhances DNA damage and mutations of cellular genes. *J. Virol.*, **78**, 8835–8843.
27. Guo,J. *et al*. (2004) Enhanced chemosensitivity to irinotecan by RNA interference-mediated down-regulation of the nuclear factor-kappaB p65 subunit. *Clin. Cancer Res.*, **10**, 3333–3341.
28. Calvisi,D.F. *et al*. (2004) Disruption of beta-catenin pathway or genomic instability define two distinct categories of liver cancer in transgenic mice. *Gastroenterology*, **126**, 1374–1386.
29. Lee,J.S. *et al*. (2004) Classification and prediction of survival in hepatocellular carcinoma by gene expression profiling. *Hepatology*, **40**, 667–676.
30. Török,N.J. *et al*. (2002) Nitric oxide inhibits apoptosis downstream of cytochrome C release by nitrosylating caspase 9. *Cancer Res.*, **62**, 1648–1653.
31. Calvisi,D.F. *et al*. (2004) Disregulation of E-cadherin in transgenic mouse models of liver cancer. *Lab. Invest.*, **84**, 1137–1147.

32. Luceri,C. *et al*. (2000) Detection of somatic DNA alterations in azoxymethane-induced F344 rat colon tumors by random amplified polymorphic DNA analysis. *Carcinogenesis*, **21**, 1753–1756.
33. Greten,F.R. *et al*. (2004) The IKK/NF-kB activation pathway-a target for prevention and treatment of cancer. *Cancer Lett.*, **206**, 193–199.
34. Favata,M.F. *et al*. (1998) Identification of a novel inhibitor of mitogen-activated protein kinase kinase. *J. Biol. Chem.*, **273**, 18623–18632.
35. Suh,S.J. *et al*. (2006) The naturally occurring bioflavonoid, ochnaflavone, inhibits LPS-induced iNOS expression, which is mediated by ERK1/2 via NF-kappa B regulation, in RAW264.7 cells. *Arch. Biochem. Biophys.*, **447**, 136–146.
36. Pahan,K. *et al*. (2000) Expression of a dominant-negative mutant of p21(ras) inhibits induction of nitric oxide synthase and activation of nuclear factor-kappaB in primary astrocytes. *J. Neurochem.*, **74**, 2288–2295.
37. Briassouli,P. *et al*. (2007) Aurora-A regulation of nuclear factor-kappaB signaling by phosphorylation of IkappaBalpha. *Cancer Res.*, **67**, 1689–1695.
38. Li,L.G. *et al*. (2005) Inducible nitric oxide synthase, nitrotyrosine and apoptosis in gastric adenocarcinomas and their correlation with a poor survival. *World J. Gastroenterol.*, **11**, 2539–2544.
39. Zhang,J. *et al*. (2005) Expressions of nuclear factor kappaB, inducible nitric oxide synthase, and vascular endothelial growth factor in adenoid cystic carcinoma of salivary glands: correlations with the angiogenesis and clinical outcome. *Clin. Cancer Res.*, **11**, 7334–7343.
40. Hoki,Y. *et al*. (2007) iNOS-dependent DNA damage in patients with malignant fibrous histiocytoma in relation to prognosis. *Cancer Sci.*, **98**, 163–168.
41. Cianchi,F. *et al*. (2004) Cyclooxygenase-2 activation mediates the proangiogenic effect of nitric oxide in colorectal cancer. *Clin. Cancer Res.*, **10**, 2694–2704.
42. Rahman,M.A. *et al*. (2001) Coexpression of inducible nitric oxide synthase and COX-2 in hepatocellular carcinoma and surrounding liver: possible involvement of COX-2 in the angiogenesis of hepatitis C virus-positive cases. *Clin. Cancer Res.*, **7**, 1325–1332.
43. Kong,G. *et al*. (2002) Role of cyclooxygenase-2 and inducible nitric oxide synthase in pancreatic cancer. *J. Gastroenterol. Hepatol.*, **17**, 914–921.
44. Ozel,E. *et al*. (2006) Expression of cyclooxygenase-2 and inducible nitric oxide synthase in ovarian surface epithelial carcinomas: is there any correlation with angiogenesis or clinicopathologic parameters? *Int. J. Gynecol. Cancer*, **16**, 549–555.
45. Ropponen,K.M. *et al*. (2000) Expression of inducible nitric oxide synthase in colorectal cancer and its association with prognosis. *Scand. J. Gastroenterol.*, **35**, 1204–1211.
46. Tschugguel,W. *et al*. (1999) Expression of inducible nitric oxide synthase in human breast cancer depends on tumor grade. *Breast Cancer Res. Treat.*, **56**, 145–151.
47. Denda,A. *et al*. (2007) Expression of inducible nitric oxide (NO) synthase but not prevention by its gene ablation of hepatocarcinogenesis with fibrosis caused by a choline-deficient, L-amino acid-defined diet in rats and mice. *Nitric Oxide*, **16**, 164–176.
48. Rai,R.M. *et al*. (1998) Impaired liver regeneration in inducible nitric oxide synthase deficient mice. *Proc. Natl Acad. Sci. USA*, **95**, 13829–13834.
49. Ghoshal,A.K. (1995) New insight into the biochemical pathology of liver in choline deficiency. *Crit. Rev. Biochem. Mol. Biol.*, **30**, 263–273.
50. Calvisi,D.F. *et al*. (2008) Ras-driven proliferation and apoptosis signaling during rat liver carcinogenesis is under genetic control. *Int. J. Cancer* in press.
51. Cai,R.L. *et al*. (2003) Segregation analysis of hepatocellular carcinoma in a moderately high-incidence area of East China. *World J. Gastroenterol.*, **9**, 2428–2432.
52. Du,O. *et al*. (2006) Regulation of human nitric oxide synthase 2 expression by Wnt beta-catenin signaling. *Cancer Res.*, **66**, 7024–7031.
53. Cadoret,A. *et al*. (2001) Hepatomegaly in transgenic mice expressing an oncogenic form of beta-catenin. *Cancer Res.*, **61**, 3245–3249.
54. Epstein,R.J. *et al*. (2007) Reversing hepatocellular carcinoma progression by using networked biological therapies. *Clin. Cancer Res.*, **13**, 11–17.

Received March 28, 2008; revised May 19, 2008; accepted June 17, 2008